EUROPEAN SYNCHROTRON RADIATION FACILITY

INSTALLATION EUROPEENNE DE RAYONNEMENT SYNCHROTRON

ESRF

Experiment Report Form

The double page inside this form is to be filled in by all users or groups of users who have had access to beam time for measurements at the ESRF.

Once completed, the report should be submitted electronically to the User Office via the User Portal:

https://wwws.esrf.fr/misapps/SMISWebClient/protected/welcome.do

Reports supporting requests for additional beam time

Reports can be submitted independently of new proposals – it is necessary simply to indicate the number of the report(s) supporting a new proposal on the proposal form.

The Review Committees reserve the right to reject new proposals from groups who have not reported on the use of beam time allocated previously.

Reports on experiments relating to long term projects

Proposers awarded beam time for a long term project are required to submit an interim report at the end of each year, irrespective of the number of shifts of beam time they have used.

Published papers

All users must give proper credit to ESRF staff members and proper mention to ESRF facilities which were essential for the results described in any ensuing publication. Further, they are obliged to send to the Joint ESRF/ ILL library the complete reference and the abstract of all papers appearing in print, and resulting from the use of the ESRF.

Should you wish to make more general comments on the experiment, please note them on the User Evaluation Form, and send both the Report and the Evaluation Form to the User Office.

Deadlines for submission of Experimental Reports

- 1st March for experiments carried out up until June of the previous year;
- 1st September for experiments carried out up until January of the same year.

Instructions for preparing your Report

- fill in a separate form for each project or series of measurements.
- type your report, in English.
- include the reference number of the proposal to which the report refers.
- make sure that the text, tables and figures fit into the space available.
- if your work is published or is in press, you may prefer to paste in the abstract, and add full reference details. If the abstract is in a language other than English, please include an English translation.

Names and affiliations of applicants (* indicates experimentalists):

*Koen Janssens, Department of Chemistry, Antwerp University, Belgium

*Letizia Monico, CNR-ISTM, Perugia, Italy/Department of Chemistry, Antwerp University, Belgium

*Frederik Vanmeert, Department of Chemistry, Antwerp University, Belgium

1. INTRODUCTION

A combination of synchrotron radiation (SR)-based micro X-ray fluorescence (µ-XRF) and X-ray absorption near edge structure (µ-XANES) spectroscopies at the Cr K-edge (exp. EC-504, EC-799, EC-1051) allowed us to established that the darkening of different chrome yellow varieties ($PbCr_{1-x}S_xO_4$, $0 \leq x \leq 0.8$; denoted below as CYs) in a number of Van Gogh paintings is ascribable to the reduction of the original chromate to Cr(III)-compounds.[1,2,3,4,5,6] Cr(III)-oxide-, sulfates-, organo metal-based compounds were identified as alteration products. We also found that orthorhombic S-rich $PbCr_{1-x}S_xO_4$ ($x \geq 0.5$) solid solutions showed a higher tendency toward photo-reduction than the monoclinic S-poor ones ($0 \leq x \leq 0.4$) and that they degraded also under exposure to the violet-blue light (*i.e.,* $400 \leq \lambda \leq 480$ nm).[4]

This alteration phenomenon make it challenging to establish the optimal museum conditions to ensure a safe display of these unique masterpieces, especially in the view of possible employment of emerging illumination devices, such as white light emitting diodes (WLEDs) devices, which are generally characterized by a considerable emission of violet-blue radiations.

Building upon knowledge acquired through previous studies,[4] these investigations (results recently published) [7], were aimed to (i) evaluate the effects of the violet-blue-green light (400-560 nm) emitted by several illumination devices and (ii) to determine the wavelength dependence of the alteration process of different CY types. Moreover, since in paintings, such as Van Gogh's *Sunflowers,* CY is often present in mixture with other pigments (some of them with well-known photo-redox properties, such as ZnO, Pb_3O_4, HgS), we also explored whether these admixture materials may influence or not the stability of CYs (results published soon).

2. EXPERIMENTAL

2.1 Experimental setup

A highly monochromatic primary beam (with $\Delta E/E = 10^{-4}$) was produced using a Si(220) fixed-exit double-crystal monochromator. The incident beam was focused with Kirkpatrick-Baez mirrors down to a diameter of 0.8×0.3 µm² (h×v) and maintained stable within 0.5 µm vertical and 0.3 µm horizontal around the Cr K-edge (5.96-6.09 keV). XRF signals were collected in the horizontal plane and at 69° with respect to the incident beam direction using a single energy-dispersive silicon drift detector (Xflash 5100, Bruker).

Lines of µ-XANES spectra were acquired in XRF mode by scanning the primary energy in the 5.96-6.09 keV range with energy step of 0.2 eV. The energy calibration was performed with respect to the first inflection point of the Cr metal foil, which was determined by its first derivative and set to 5.989 keV. The software ATHENA,[8] was used to perform the normalization and to carry out a linear combination fitting of the

XANES spectra against a library of profiles of Cr-reference compounds. This procedure allowed for quantitatively estimating the percentage relative amount of Cr(VI) and Cr(III) species (expressed as [Cr(VI)]/[Cr$_{total}$] and [Cr(III)]/[Cr$_{total}$]) as a function of the depth.

During the μ-XRF mapping experiments, the fluorescence signals were generated by employing a monochromatic primary beam of fixed energy (around the Cr K-edge). Maps of the same area were recorded using 100 ms/pixel at two different excitation energies: (a) at 5.993 keV, for favoring the excitation of the Cr(VI)-species and (b) at 6.088 keV to obtain the fluorescence intensity of all Cr-species. The software PyMca was used to fit the fluorescence spectra and separate the different elemental contributions.[9]

2.2 Preparation of paint models

Powders of monoclinic PbCrO$_4$ (S$^*_{1mono}$) and mainly orthorhombic PbCr$_{0.2}$S$_{0.8}$O$_4$ (S$^*_{3D}$) were synthesized as described in our previous work.[**Errore. Il segnalibro non è definito.**] The asterisk denotes the pure powders, not yet mixed with the organic binder. Paint models (S$_{1mono}$, S$_{3D}$) were prepared by mixing these powders with linseed oil in a 4:1 mass ratio and by applying the mixture on polycarbonate slides.

Additional paint models were obtained by mixing either S$^*_{1mono}$ or S$^*_{3D}$ with an admixture pigment such as vermilion (HgS), emerald green [Cu(C$_2$H$_3$O$_2$)$_2$·3Cu(AsO$_2$)$_2$], minium (Pb$_3$O$_4$) (10 wt.%) or zinc white (50 and 90 wt.%). All samples were analyzed as thin sections (5-10 μm thickness).

2.3 Artificially aging experiments

2.3.1. Aging with commercial lamps.

Three pc-WLEDs devices (below denoted as "LED 1$_{warm-white}$", "LED 2$_{very-warm-white}$", "LED 3$_{daylight-white}$"), one halogen light and an UV-filtered xenon lamp were used for the treatment of a series of S$_{1mono}$ and S$_{3D}$ paints. These ligth sources were selected due to their different emission in the violet-blue-green visible light range. Paints with admixture pigments were only exposed to the UV-filtered xenon lamp.

"High-flux" experiments were conducted by keeping illuminance values at the sample position between 1.7-2.9 $\times 10^5$ lux; paints were irradiated for a variable number of hours (between 70-115 hours) to obtain an equivalent final luminous exposure. In order to evaluate any flux-dependence of the degradation process, equivalent aging tests were also performed under "low-flux" conditions for 1 months, with an illuminance approximately decreased by a 10^3 factor.

2.3.2. Aging with monochromatic light.

A series of S$_{3D}$ paints were irradiated using a xenon lamp equipped with a monochromator for selecting appropriate wavelengths range. Experiments were conducted in the 288-560 nm range, with 4-5 W/m^2 average irradiance and for a variable number of hours to obtain an equivalent number of total incident photon counts (about 6-7$\times 10^{24}$ ph·m^{-2}·nm^{-1}; *cf.* Figure 3A).

3. RESULTS

3.1 Aging with commercial lamps

In Figure 1A the photographs of S_{1mono} (PbCrO$_4$) and S_{3D} (PbCr$_{0.2}$S$_{0.8}$O$_4$) paints before and after "high-flux" exposure to different commercial lamps are compared. In particular for S_{3D} the darkening depends on the type of employed illumination systems. In agreement with our previous experiments,[4] S_{1mono} samples do not reveal the same profound darkening as do S_{3D} paints, where the alteration is present as a thicker layer of about 4-5 µm (*cf.* photomicrographs of Figure 1B). Figure 2 shows the Cr chemical state maps acquired from light-exposed S_{3D} thin sections.

The data-sets collected from aged S_{1mono} paints showed slight and similar changes regardless of the employed illumination systems: a Cr(III) relative amount not higher than 10-15% was detected at the surface (spectra not reported). Thus, in Figure 2 only the results obtained from the aged S_{3D} samples are presented.

Regarding "high-flux" experiments, S_{3D} paints exposed either to LED 1$_{warm-white}$" or "LED 3$_{daylight-white}$" show the presence of a superficial Cr(III)-rich layer of 3-4 µm in thickness, while Cr(VI)-species are the main constituents of the yellow paint underneath. A similar distribution can be observed after aging with the "halogen" and the "UV-filtered xenon" lamps. The sample irradiated using "LED 2$_{very-warm-white}$" reveals the presence of Cr(III)-species at the surface as well, but in lower amount than other paints.

Lines of Cr K-edge XANES spectra collected along the exposed surface of S_{3D} samples (data not shown) confirm the reduction of the original Cr(VI); this is demonstrated by a decrease of the Cr pre-edge peak intensity at 5.993 keV and the absorption edge shift toward lower energies.[1,4] These changes are more pronounced in the spectra collected in the upper 1-3 µm of the thin sections and after aging with the "halogen" and "UV-filtered xenon" lamps.

In line with our previous studies,[4] three fitting components, such as PbCr$_{0.2}$S$_{0.8}$O$_4$, Cr (III)-oxides [*i.e.,* Cr(OH)$_3$/Cr$_2$O$_3$] and either Cr(III) acetate [(CH$_3$CO$_2$)$_7$Cr$_3$(OH)$_2$], or Cr(III) acetylacetonate [Cr(C$_5$H$_7$O$_2$)$_3$], or Cr$_2$(SO$_4$)$_3$·H$_2$O were necessary to obtain a good description of the XANES spectra recorded along the first 1-3 µm of each thin section. Only two components [PbCr$_{0.2}$S$_{0.8}$O$_4$ and Cr(III)-oxides/Cr(III) organo metal-based compounds/Cr$_2$(SO$_4$)$_3$·H$_2$O] were required to fit the profiles recorded at greater depth. However, regardless of which components were used, the fitting models yielded comparable [Cr(III)]/[Cr$_{total}$] values (results not reported in detail).

As Figure 2 shows, the fraction of Cr(III)-species at the surface decreases going from the paints aged either with "halogen" or "UV-filtered xenon" lamps (≈55%) to that irradiated with "LED 2 $_{very-warm-white}$" (≈30%). The abundance of reduced Cr was about 35% for the samples irradiated with "LED 1$_{warm-white}$" and "LED
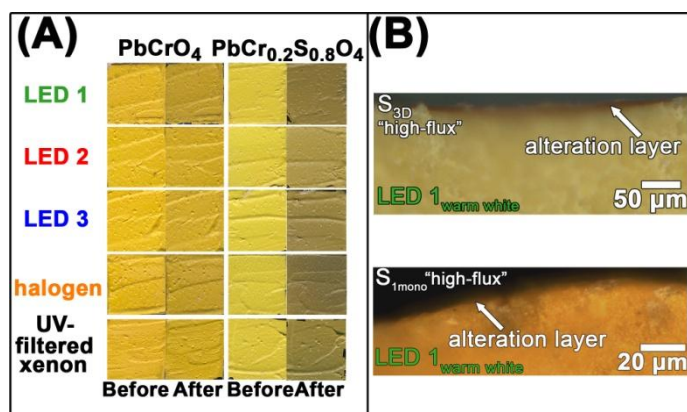

Figure 1. (A) Photographs of S_{1mono} (PbCrO$_4$) and S_{3D} (PbCr$_{0.2}$S$_{0.8}$O$_4$) paints before and after "high-flux" exposure to different lamps. (B) Microphotograph of (top) S_{3D} and (bottom) S_{1mono} thin sections aged using "LED 1$_{warm-white}$" at "high-flux".

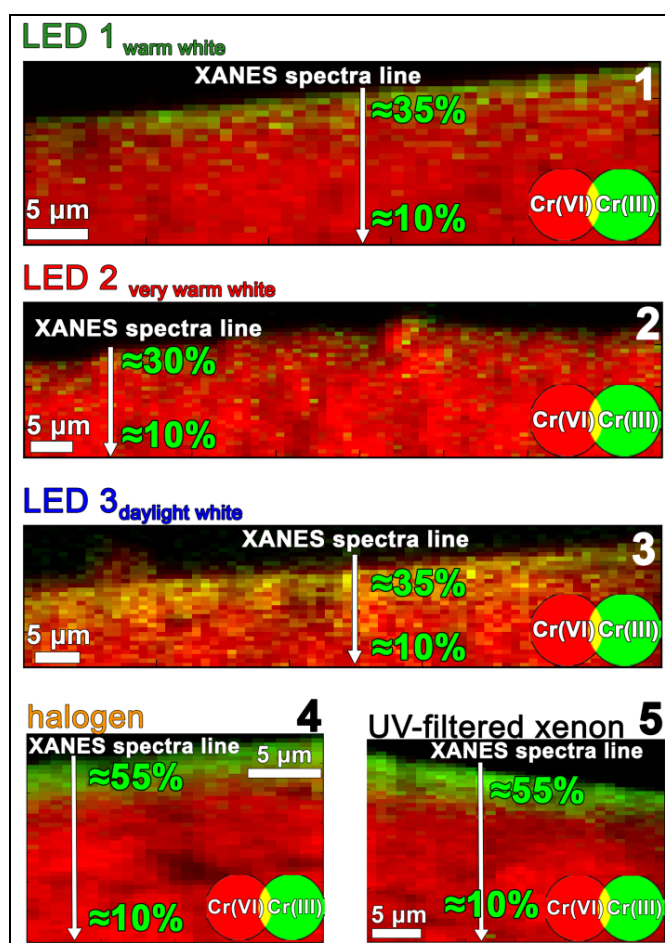**Figure 2.** RG Cr(VI)/Cr(III) chemical state maps obtained from S_{3D} after "high-flux" exposure to different lamps [step sizes (h×v): 0.8×0.3 µm^2; dwell time: 100 ms/pixel]. Green labels indicates the fraction of Cr(III)-species obtained from the linear combination fitting of the line of Cr K-edge XANES spectra collected in correspondence of the areas indicated by white arrows.

3$_{daylight-white}$". For all samples, the fraction of Cr(III)-compounds progressively decreases with increasing depth down to values of 5-10 %.

After "low-flux" aging, Cr(VI)/Cr(III) depth profiles (data not reported) do show a similar trend as revealed "high-flux" experiments, but with lower abundance of Cr(III) at the surface (about 20-25%).

On the basis of these results, the photo-response of S$_{3D}$ toward different lamps cannot be explained only by considering the emission of each illumination devices in the range of maximum absorption of S$_{3D}$ (*i.e.*, 400-460 nm). In fact, despite "LED 1$_{warm-white}$" shows a lower total emission than "LED 3$_{daylight-white}$" in this region, the two systems yielded to comparable darkening. Similarly, the significant influence of the halogen lamp on the reduction process (*i.e.,* comparable to that of the "UV-filtered xenon" device) cannot be justified on the basis of its emission profile in the 400-460 nm range. This observation suggests that also other wavelength bands of the visible light might activate the darkening process. This aspect is analyzed in more detail in the following section by describing the results obtained from a series of S$_{3D}$ paints that were aged using a selection of UV-Vis light wavelengths.

3.2. Aging with monochromatic light

In Figure 3A, the photographs of S$_{3D}$ paints after exposure to different wavelengths are shown. The darkening is visible for all paints and it becomes progressively less significant for aging wavelengths above 500 nm. Figures 3B shows a selection of the Cr chemical states maps obtained from the S$_{3D}$ paints aged at 288 nm and 500 nm. The Cr(III)-amount decreases with increasing depth (down to 5-10%) and its different values at the surface depend on the employed aging wavelength. After exposure at 288 nm, the formation of a superficial 5 µm thick layer composed of about 45% of
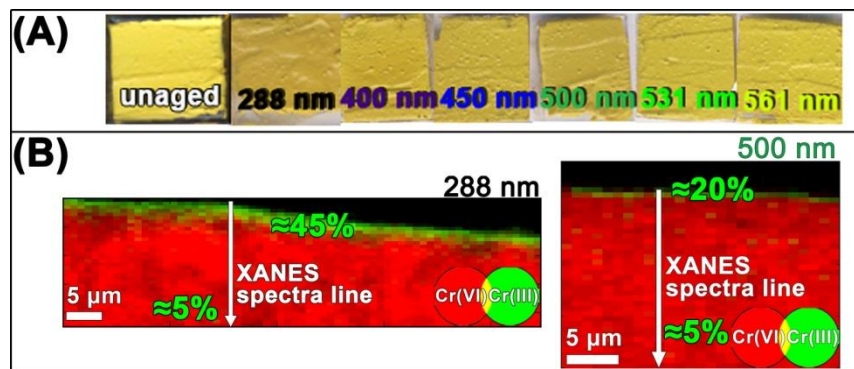

Figure 3. (A) Photographs of S$_{3D}$ paints before and after exposure to monochromatic lights. (B) RG Cr(VI)/Cr(III) chemical state maps obtained from S$_{3D}$ paints after exposure at 288 nm and 500 nm [step sizes (h×v): 0.8×0.3 µm^2; dwell time: 100 ms/pixel]. Green labels indicates the fraction of Cr(III)-species obtained from the linear combination fitting of the line of Cr K-edge XANES spectra collected in correspondence of the regions indicated by white arrows.

Cr(III) is observed (Figures 3B, left side). Cr(III)-species in amount at about 25% and 20%, were also found within the upper 5 µm of the samples aged at 400 and 450 nm, respectively (results not shown). The exposure at 500 and 531 nm yielded the formation of a 2-3 µm thick superficial layer, that contains about 20% of Cr(III)-compounds (Figures 3B, right side). After aging at 561 nm (results not reported), these alteration products reach an abundance at around 10-15%. The efficiency both of the 500 nm and 400 nm radiations to the darkening/Cr reduction can provide an explanation for the S$_{3D}$ response toward exposure to different commercial lamps (see par. "3.1 Aging with commercial lamps").

3.3. Aging of different CYs types with admixture pigments

In Figure 4A, the photographs of S$_{1mono}$ and S$_{3D}$ paints mixed with emerald green, vermilion, minium or zinc white before and after exposure to the UV-filtered xenon lamp are shown.

Before aging, the presence of admixture pigments change with less extent the color shade of the paints with respect to those containing only chrome yellow (denoted as "pure" in Figure 4A); the tone also depends on the lead chromate-based pigment varieties. After light exposure, the color change depends on the type of admixture pigment. In line with previous experiments [1,4] and as above-mentioned, S$_{3D}$-based samples show a stronger darkening with respect to S$_{1mono}$-based ones.

Regaring Cr-speciation results, the data-sets collected from aged S$_{1mono}$-based paints showed similar changes regardless to the admixture pigments: a Cr(III) relative amount not higher than 10-15% was detected at the surface. Thus, in Figure 4 only the results obtained from the aged S$_{3D}$-based samples are presented and described in detail.

Figures 4B-C shows a selection of the Cr chemical states maps obtained from the aged S$_{3D}$-based paints and the corresponding XANES profiles collected at the paint surface.

As observed for the "pure paint" (*cf.* Figures 2), in all samples, the formation of a superficial 3-5 μm thick layer is observable (Figure 4B). The fraction of Cr(III) decreases with increasing depth (down to 5-10%; results not shown) and its different values at the surface depend on the nature of the admixture pigment. In particular, the Cr(III)-amount decreases going from the aged paints mixed either with "vermilion" (≈55%) or "emerald green" (≈45%) to that containing "minium" (≈30%) (Figures 4C; light red, dark red and green lines). Its abundance reaches values at around 20-25% for the paints containing Zn white (Figures 4C; blue and cyan lines).
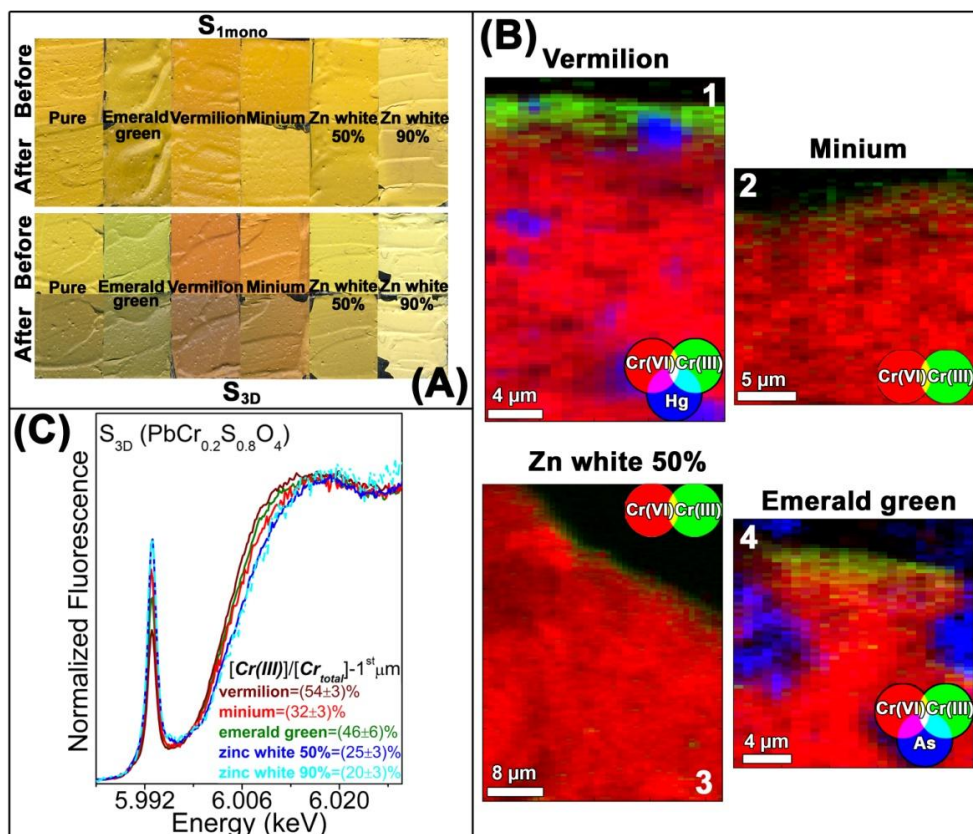

Figure 4. (A) Photographs of paint models with different admixture pigments before and after aging with UV-filtered xenon lamp. (B) RG Cr(VI)/Cr(III) chemical state maps obtained from aged S$_{3D}$ paints mixed with (1) vermilion, (2) minium, (3) Zn white and (4) emerald green [step sizes (h×v): 0.8×0.3 μm^2; dwell time: 100 ms/pixel]. In (B1) and (B4) maps of Hg and As are reported in blue color. (C) XANES profiles and corresponding Cr(III) abundance obtained as average of the data recorded from the upper first micrometer of the surface of the thin sections shown in (B)

These results suggest that the studied admixture pigments have no effect or decrease with a different extent the tendency toward reduction of the more light-sensitive CY pigment.

REFERENCES

[1] Monico, L.; Van der Snickt, G.; Janssens, K.; De Nolf, W.; Miliani, C.;Verbeeck, J.; Tian, H.; Tan, H.; Dik, J.; Radepont, M.; Cotte, M. *Anal. Chem.* **2011**, *83*, 1214-1223.

[2] Monico, L.; Van der Snickt, G.; Janssens, K.; De Nolf, W.; Miliani, C.; Dik, J.; Radepont, M.; Hendriks, E.; Geldof, M.; Cotte, M. *Anal. Chem.* **2011**, *83*, 1224-1231.

[3] Monico, L.; Janssens, K.; Miliani, C.; Brunetti, B. G.; Vagnini, M.; Vanmeert, F.; Falkenberg, G.; Abakumov, A.; Lu, Y.; Tian, H.; Verbeeck, J.; Radepont, M.; Cotte, M.; Hendriks, E.; Geldof, M.; van der Loeff, L.; Salvant, J.; Menu, M. *Anal. Chem.* **2013**, *85*, 851-859.

[4] Monico, L.; Janssens, K.; Miliani, C.; Van der Snickt, G.; Brunetti, B. G.; Cestelli Guidi, M.; Radepont, M.; Cotte, M. *Anal. Chem.* **2013**, *85*, 860-867.

[5] Monico, L.; Janssens, K.; Vanmeert, F.; Cotte, M.; Brunetti, B. G.; Van der Snickt, G.; Leeuwestein, M.; Salvant Plisson, J.; Menu, M.; Miliani, C. *Anal. Chem.* **2014**, *86*, 10804-10811.

[6] Monico, L.; Janssens, K.; Alfeld, M.; Cotte, M.; Vanmeert, F.; Ryan, C. G.; Falkenberg, G.;. Howard, D. L.; Brunetti, B. G.; Miliani, C. *J. Anal. At. Spectrom.* **2015**, *30*, 613-626.

[7] Monico, L.; Janssens, K.; Cotte, M.; Romani, A.; Sorace, L.; Grazia, C.; Brunetti, B. G.; Miliani, C. *J. Anal. At. Spectrom.* **2015**, *30*, 1500-1510.

[8] Ravel, B.; Newville, M. *J. Synchrotron Radiat.* **2005**, *12,* 537–541.

[9] Solé, V. A.; Papillon, E.; Cotte, M.; Walter, P.; Susini, J. *Spectrochim. Acta B* **2007**, *62*, 63–68.